

Portland State University

PDXScholar

Mathematics and Statistics Faculty
Publications and Presentations

Fariborz Maseeh Department of Mathematics
and Statistics

6-2015

Dynamics of Locally Coupled Oscillators with Next-Nearest-Neighbor Interaction

J. Herbrych
University of Crete

A. G. Chazirakis
University of Crete

N. Christakis
University of Crete

J. J. P. Veerman
Portland State University, veerman@pdx.edu

Follow this and additional works at: https://pdxscholar.library.pdx.edu/mth_fac



Part of the [Dynamic Systems Commons](#)

Let us know how access to this document benefits you.

Citation Details

Herbrych, J., Chazirakis, A. G., Christakis, N., & Veerman, J. J. P. (2015). Dynamics of locally coupled oscillators with next-nearest-neighbor interaction. arXiv preprint arXiv:1506.07381.

This Pre-Print is brought to you for free and open access. It has been accepted for inclusion in Mathematics and Statistics Faculty Publications and Presentations by an authorized administrator of PDXScholar. Please contact us if we can make this document more accessible: pdxscholar@pdx.edu.

Dynamics of locally coupled oscillators with next–nearest–neighbor interaction

J. Herbrych^{1,2}, A. G. Chazirakis³, N. Christakis^{1,2}, and
J. J. P. Veerman^{1,2,4}

¹Crete Center for Quantum Complexity and Nanotechnology, University of Crete,
P.O. Box 2208, 71003 Heraklion, Greece

²Department of Physics, University of Crete, P.O. Box 2208, 71003 Heraklion, Greece

³Department of Mathematics and Applied Mathematics, University of Crete, 71409
Heraklion, Greece

⁴Fariborz Maseeh Department of Mathematics and Statistics, Portland State
University, Portland, OR, USA

E-mail: jacek@physics.uoc.gr, veerman@pdx.edu

May 2015

Abstract. A theoretical description of decentralized dynamics within linearly coupled, one–dimensional oscillators (agents) with up to next–nearest–neighbor interaction is given. Conditions for stability of such system are presented. Our results indicate that the stable systems have response that grow at least linearly in the system size. We give criteria when this is the case. The dynamics of these systems can be described with traveling waves with strong damping in the high frequencies. Depending on the system parameters, two types of solutions have been found: damped oscillations and reflectionless waves. The latter is a novel result and a feature of systems with at least next–nearest–neighbor interactions. Analytical predictions are tested in numerical simulations.

PACS numbers: 05.45.Pq, 07.07.Tw, 45.30.+s, 73.21.Ac

Keywords: Dynamical Systems, Chaotic Dynamics, Optimization and Control, Multiagent Systems

Submitted to: *J. Phys. A: Math. Theor.*

1. Introduction

Linearly coupled oscillators play an important role in almost all areas of science and technology (see Introduction of Ref. [1]). The phenomena of coupled systems appear on all length– and time–scales. From synchronization of power generators in power–grid networks [2, 3], through the traffic control of vehicular platoons [4, 5, 6, 7, 8, 9], collective

decision-making in biological systems [10, 11, 12, 13, 14] (e.g., transfer of long-range information in flocks of birds), to the atomic scale lattice vibrations (so-called phonons), just to name few of them. The nature of communication within such a system crucially influences the behaviour of it. In the presence of centralized information, like global damping or knowledge of the desired velocity, the performance of many of these systems is good [4, 7, 8] in the sense that the trajectories of the agents quickly converge to coherent (or synchronized) motion [see Equation (1)]. On the other hand, convergence to coherent motion in decentralized systems is much less obvious, since no overall goal is observed by all agents. In this case, the only available observations (i.e., position and velocity) are relative to the agent. The complication of the problem is even greater if information is locally exchanged by agents in a neighborhood that is small in comparison to the system size.

It is therefore of significant importance to develop a theory that deals with systems where agents may interact with few nearby agents. Although such a setup can be described by a set of linear, first order differential equations, solutions of it are nontrivial. For example, it is well known [15, 16] that the transients analysis of a system of the form $\dot{z} = Mz$ is extremely difficult unless the square matrix M is normal, i.e., eigenvectors form a normal basis. In systems that are not normal the spectrum of M only gives information about the behavior of the trajectories as $t \rightarrow \infty$ (where t is the time). In course of convergence, amplitudes of transient oscillations can still grow exponentially with system size (number of agents). It is obvious that the latter is not desired for real applications. Here, we utilize the mathematical conjectures given in References [17] and [18] and describe the set of parameter values such that the dynamics of the whole system is described essentially by traveling waves (excitation in the physics language). Within such a setup, transient parameters grow linearly with the system size.

In this work, we present the theoretical basis for modeling linear, one-dimensional (1D) systems of many agents, where up to next-nearest-neighbor (NNN) interactions are allowed. The developed theory is general and is not limited to symmetric interactions as is common in physics (see Chapter 21 and 22 in Ref. [19]). The circular system with periodic boundary conditions is used as the basis in order to derive all necessary stability conditions and quantities which describe the wave-like behaviour. Once the formulation is completed, the theory is numerically tested for a system on the line, where rigorous statements are hard or even not possible. Simulations in a parallel computing environment are carried out in order to verify the results for various system configurations and different boundary conditions. Furthermore, a new type of solution, so-called reflectionless waves, was discovered.

The paper is organized as follows. In Section 2 we define the model of interacting agents. The main method is described in Section 3. In Section 4 we give basic stability conditions together with analytical expressions for signal velocities of wave-like propagation. Section 5 is devoted to Routh-Hurwitz stability criteria. The classification of solutions is given in Section 6. This includes the description of the reflectionless waves on the line, which to the best of our knowledge is a new result. In fact we find a third type

of solutions on the circle, but these do not result in solutions on the line. Numerical tests and error analysis are given in Section 7. Finally, our main conclusions are summarized in Section 8.

2. The NNN system of coupled agents

We consider a model of an 1D array of N decentralized agents (linearly damped harmonic oscillators) on the line, interacting with nearest- and next-nearest-neighbors. At time $t \leq 0$ the agents are in equilibrium (for some a priori fixed $\Delta > 0$)

$$x_k = -\Delta k,$$

for $k \in \{1, \dots, N\}$. Here a_0 , b_0 and Δ are real constants. Then for $t > 0$ the leader starts moving forward at velocity v_0 :

$$\forall t \geq 0 \quad x_0(t) = v_0 t.$$

Note that the leader is not influenced by other agents, although other agents ($k = 1$ and $k = 2$) are influenced by it.

Coherent motion is defined as:

$$x_k = a_0 t + b_0 - \Delta k, \tag{1}$$

where a_0 and b_0 are arbitrary real constants. Our aim is not only to find systems whose trajectories converge to coherent motion, but also to find those systems whose convergence is quick and whose transients are small. In fact we will show that we can choose the parameters so that convergence to coherent solutions takes place in times of order $t \sim \mathcal{O}(N)$ and that the transients also grow as $\mathcal{O}(N)$. Such performance can not be improved for the type of the systems studied in this work.

The general decentralized flock with next-nearest-neighbor interaction can be linearized by setting $z_k \equiv x_k - v_0 t + \Delta k$. Note that in these (z_k) coordinates the leader is stationary when $t > 0$. The equations of motion for the new variables z_k can be written as [20]:

$$\ddot{z}_k = \sum_{j=-2, j \neq 0}^2 [p_j (z_k - z_{k-j}) + v_j (\dot{z}_k - \dot{z}_{k-j})], \tag{2}$$

where p_j is position and v_j is velocity. Note that in the above equation the right hand side consists of positions and velocities that are relative to the agent. In order to further simplify the notation, we introduce constant $g_x \equiv \sum_j p_j$, define $\rho_{x,0} = 1$, and for all other values $j = -2, -1, 1, 2$ set $\rho_{x,j} = p_j/g_x$. In similar fashion we define g_v and $\rho_{v,j}$ for the velocity coefficient v_j . See Figure 1 for a sketch of the information flow.

In this notation, the equation of motion of the flock in \mathbb{R} becomes:

Definition 2.1. *The equations of motion of the NNN system with $N > 4$ agents are (for $k \in \{1, \dots, n\}$):*

$$\ddot{z}_k = \sum_{j=-2}^2 (g_x \rho_{x,j} z_{k+j} + g_v \rho_{v,j} \dot{z}_{k+j}). \tag{3}$$

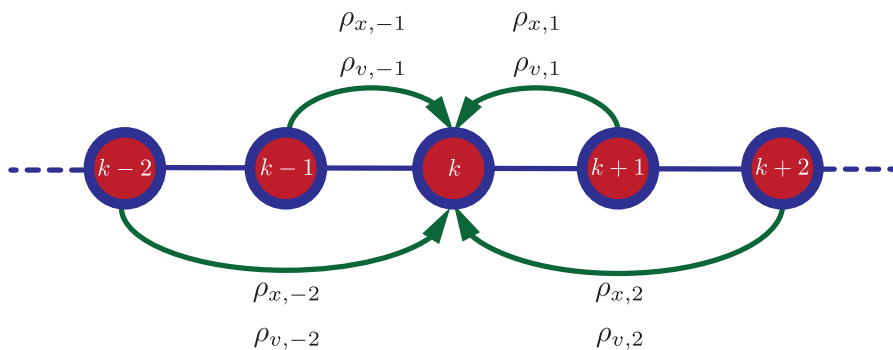


Figure 1. Sketch of information flow. Available information about position $\rho_{x,j}$ and velocity $\rho_{v,j}$ of nearest $j = k \pm 1$ and next-nearest $j = k \pm 2$ agents for k 'th agent. Exception from this are boundary agents $k = 1, N - 1, N$ on which we comment later.

This system is subject to the constraints

$$\rho_{x,0} = \rho_{v,0} = 1, \quad \sum_{j=-2}^2 \rho_{x,j} = \sum_{j=-2}^2 \rho_{v,j} = 0, \quad (4)$$

and to the conditions:

$$k > 0 : z_k(0) = 0, \quad \dot{z}_k(0) = -v_0 \quad \text{and} \quad t \geq 0 : z_0(t) = 0. \quad (5)$$

Finally, z_1, z_{N-1} , and z_N are subject to boundary conditions discussed in the end of this section. From now on we denote this system by \mathcal{S}_N , and also the collection of the systems $\{\mathcal{S}_N\}_{N>4}$ by \mathcal{S} .

In view of these constraints, this is effectively an 8-parameter family of systems of (variable) size N . Notice also that Equation (4) is a consequence of the decentralized system, where the locality of exchange of information is expressed by the fact that index j in Equation (3) runs over the four nearest neighbors.

Now we use vector notation and write $z \equiv (z_1, z_2, z_3, \dots, z_N)^T$ together with $\dot{z} \equiv (\dot{z}_1, \dot{z}_2, \dot{z}_3, \dots, \dot{z}_N)^T$. Equation (3) may be rewritten as a first order system in $2N$ dimensions:

$$\frac{d}{dt} \begin{pmatrix} z \\ \dot{z} \end{pmatrix} = \begin{pmatrix} 0 & I \\ g_x L_x & g_v L_v \end{pmatrix} + \begin{pmatrix} 0 \\ F(t) \end{pmatrix} \equiv M_N \begin{pmatrix} z \\ \dot{z} \end{pmatrix} + \begin{pmatrix} 0 \\ F(t) \end{pmatrix}, \quad (6)$$

where $L_x, L_v \in \mathbb{R}^{N \times N}$ are matrices - the *Laplacians* - with standard definition

$$(L_x z)_k = \sum_{j=-2}^2 g_x \rho_{x,j} z_{k+j}, \quad (L_v \dot{z})_k = \sum_{j=-2}^2 g_v \rho_{v,j} \dot{z}_{k+j}, \quad (7)$$

with modifications when $k \in \{1, N - 1, N\}$ and $F(t)$ is the external force that describes the influence of the leader over its immediate neighbors.

The definition of the system is not yet complete. We will introduce two sets of boundary conditions for \mathcal{S}_N (the system on the line). We will perform numerics with both types of boundary conditions (see Section 7), in order to support our conclusion that for stable and flock stable systems the trajectories are independent of the boundary conditions.

Definition 2.2. Let \mathcal{S}_N be the linearized system in Definition 2.1. The boundary conditions are expressed in the equation for \ddot{z}_k for $k = 1, N - 1$ and N 'th agents. To this end, we will consider two nontrivial BC:

(i) *fixed interaction BC:*

$$\begin{aligned}
\ddot{z}_1 &= (g_x \rho_{x,-1} z_0 + g_v \rho_{v,-1} \dot{z}_0) \\
&\quad - [g_x (\rho_{x,-1} + \rho_{x,1} + \rho_{x,2}) z_1 + g_v (\rho_{v,-1} + \rho_{v,1} + \rho_{v,2}) \dot{z}_1] \\
&\quad + \sum_{j=1}^2 (g_x \rho_{x,j} z_{1+j} + g_v \rho_{v,j} \dot{z}_{1+j}) , \\
\ddot{z}_{N-1} &= \sum_{j=-2}^{-1} (g_x \rho_{x,j} z_{N-1+j} + g_v \rho_{v,j} \dot{z}_{N-1+j}) \\
&\quad - [g_x (\rho_{x,-2} + \rho_{x,-1} + \rho_{x,1}) z_{N-1} + g_v (\rho_{v,-2} + \rho_{v,-1} + \rho_{v,1}) \dot{z}_{N-1}] \\
&\quad + (g_x \rho_{x,1} z_N + g_v \rho_{v,1} \dot{z}_N) , \\
\ddot{z}_N &= \sum_{j=-2}^{-1} (g_x \rho_{x,j} z_{N+j} + g_v \rho_{v,j} \dot{z}_{N+j}) \\
&\quad - [g_x (\rho_{x,-2} + \rho_{x,-1}) z_N + g_v (\rho_{v,-2} + \rho_{v,-1}) \dot{z}_N] . \tag{8}
\end{aligned}$$

(ii) *fixed mass BC:*

$$\begin{aligned}
\ddot{z}_1 &= [g_x (\rho_{x,-2} + \rho_{x,-1}) z_0 + g_v (\rho_{v,-2} + \rho_{v,-1}) \dot{z}_0] \\
&\quad + \sum_{j=0}^2 (g_x \rho_{x,j} z_{1+j} + g_v \rho_{v,j} \dot{z}_{1+j}) , \\
\ddot{z}_{N-1} &= \sum_{j=-2}^0 (g_x \rho_{x,j} z_{N-1+j} + g_v \rho_{v,j} \dot{z}_{N-1+j}) \\
&\quad + [g_x (\rho_{x,1} + \rho_{x,2}) z_N + g_v (\rho_{v,1} + \rho_{v,2}) \dot{z}_N] , \\
\ddot{z}_N &= \sum_{j=-2}^0 (g_x \rho_{x,j} z_{N+j} + g_v \rho_{v,j} \dot{z}_{N+j}) \\
&\quad + [g_x (\rho_{x,1} + \rho_{x,2}) z_N + g_v (\rho_{v,1} + \rho_{v,2}) \dot{z}_N] . \tag{9}
\end{aligned}$$

In the decentralized systems the row sum of the Laplacians equals 0, $\sum_j \rho_{x,j} = \sum_j \rho_{v,j} = 0$. This implies that for the system \mathcal{S}_N boundary agents $k = 1, N - 1, N$ ρ 's have to be modified. In the case of fixed interaction BC the masses, $\rho_{x,0}$ and $\rho_{v,0}$, of the agent are not equal 1, instead it is the sum of existing interactions. On the other hand, in fixed mass BC we change the interactions of existing agents and keep the central $\rho_{x,0}$ and $\rho_{v,0}$ equal to 1.

3. Method

As stated before, the analysis of the system of Definition 2.1 is very difficult because the Laplacians given in Equation (7) are not necessarily simultaneously diagonalizable.

However, if we impose that the communication structure is not a line graph but a circular graph, the resulting Laplacians L^* become *circulant matrices*. Circulant matrices are diagonalized by the discrete Fourier transform and therefore are simultaneously diagonalizable.

Our treatment follows that of Reference [18] where using reasonable conjectures it is shown that (for nearest neighbor systems) a circular system and a system on the line evolve in a similar manner. The second step is to analyze the circular system and apply the conclusions to the systems on the line. We note here that this treatment implies that the BC on the agents labelled $k = 1, N - 1$ and N , do not enter the analysis, and therefore that these BC do not affect our conclusions. Here we do not discuss the conjectures; we briefly outline how the evolution of the two systems can be compared. We do this by stating the two main ideas involved in this.

First we need to remind the reader of the two notions of stability that play a crucial role in our analysis.

Definition 3.1. *For given N , the system \mathcal{S}_N is asymptotically stable if, given any initial condition, the trajectories always converge to a coherent motion and the convergence is exponential in time. This is equivalent to: M_N has one eigenvalue zero with multiplicity 2, and all other eigenvalues have real part (strictly) less than 0.*

Flock stability was introduced in Reference [18]:

Definition 3.2. *The collection \mathcal{S} is called flock stable if the \mathcal{S}_N are asymptotically stable for all N and if $\max_{t \in \mathbb{R}} |z_N(t)|$ grows sub-exponentially in N .*

Note that asymptotic stability is different from flock stability, the former deals with the growth of the response of a single system for N fixed, while the latter deals with the growth of the response of a sequence of systems as N tends to infinity.

The first idea is that, if the system on the line is stable and flock stable, then the behavior of the two systems away from the boundary should be the same. This is similar to what is commonly known in solid state physics as *periodic boundary conditions* (see Chapter 21 in Ref. [19]), though not exactly the same. We need this principle to apply in more generality than is usual in physics, because we are considering systems that are not symmetric and are not Hamiltonian. In extending the principle, we need to be aware that new phenomena may appear (see Section 6) and indeed its validity is not guaranteed, and needs to be checked (see Section 7). The second idea involved in this analysis is the assumption that if the system on the circle is asymptotically unstable, then the system on the line is either asymptotically unstable or flock unstable. These two ideas follow from more detailed conjectures discussed in References [17] and [18].

Recall that our real interest lies in the system on the line with N agents (plus a leader) with nontrivial BC (see sketch of dynamics presented in Figure 2).

Definition 3.3. *The equations of motion of the system with periodic boundary*

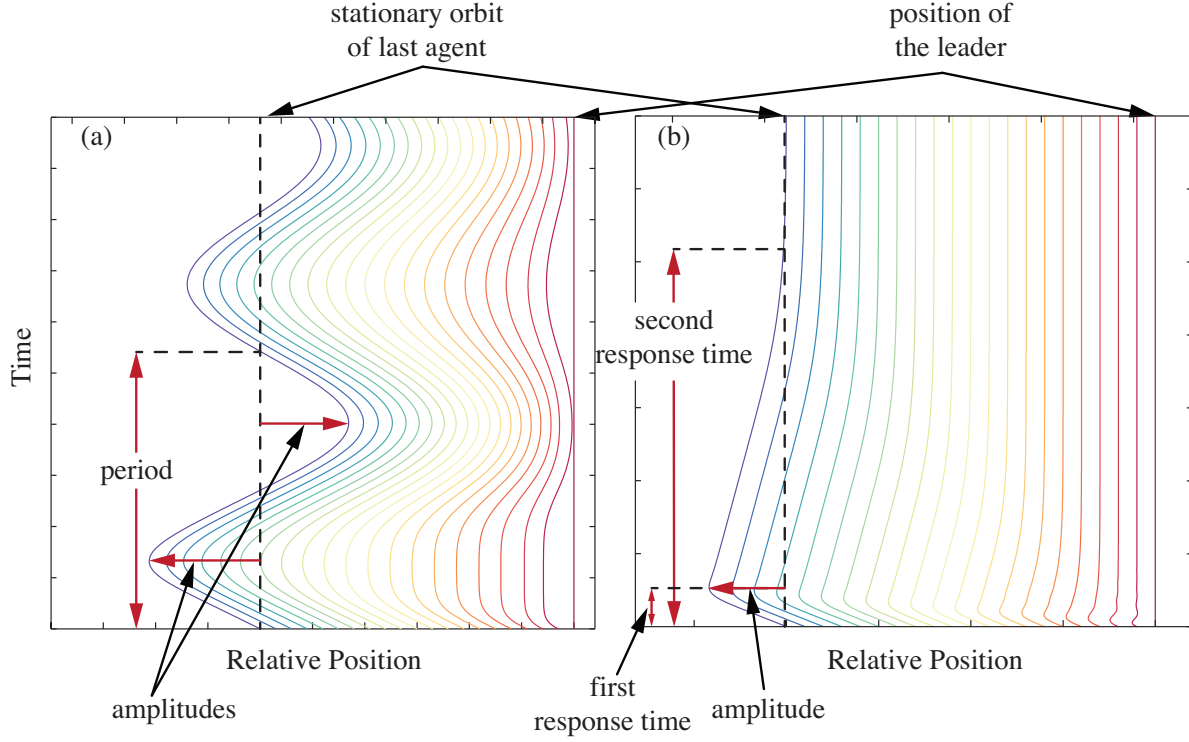


Figure 2. Dynamics of locally coupled arrays. Sketch of time-dependent dynamics of locally coupled oscillators on the line (system \mathcal{S}_N) of (a) Type I and (b) Type II (see Section 6 for detailed analysis of these solutions). x -axis depicts relative position with respect to the leader.

conditions (PBC) are:

$$\ddot{z}_k = \sum_{j=-2}^2 (g_x \rho_{x,j} z_{k+j} + g_v \rho_{v,j} \dot{z}_{k+j}).$$

This system is subject to the constraints

$$\rho_{x,0} = \rho_{v,0} = 1, \quad \sum_{j=-2}^2 \rho_{x,j} = \sum_{j=-2}^2 \rho_{v,j} = 0,$$

and to the conditions:

$$k > 0 : z_k(0) = 0, \quad \dot{z}_k(0) = -v_0, \quad \text{and } t \geq 0 : z_0(t) = 0.$$

Finally, instead of boundary conditions for z_1 , z_{N-1} , and z_N , we set:

$$\forall j \quad z_{N+j} = z_j.$$

From now on we denote this system by \mathcal{S}_N^* , and also the collection of the systems $\{\mathcal{S}_N^*\}_{N>4}$ by \mathcal{S}^* .

Definition 3.4. In order to simplify notation, we set $\alpha_{x,0} = \alpha_{v,0} = 1$ and $\beta_{x,0} = \beta_{v,0} = 0$. For $j > 0$ we have:

$$\begin{aligned} \alpha_{x,j} &= \rho_{x,j} + \rho_{x,-j}, & \beta_{x,j} &= \rho_{x,j} - \rho_{x,-j}, \\ \alpha_{v,j} &= \rho_{v,j} + \rho_{v,-j}, & \beta_{v,j} &= \rho_{v,j} - \rho_{v,-j}. \end{aligned} \tag{10}$$

Note that the sum of the α 's equals 0 through Equation (4).

We now turn to the study of the stability of the systems in \mathcal{S}^* . The Laplacians L^* now become circulant matrices and are both diagonalizable by the discrete Fourier transform. Let w_m be the m 'th eigenvector of L^* 's, that is the vector whose j 'th component satisfies:

$$(w_m)_j = \exp\left(\imath \frac{2\pi m}{N} j\right) \equiv \exp(\imath \phi j), \quad (11)$$

with the obvious definition of ϕ . We denote the m 'th eigenvalues of $g_x L_x^*$ by $\lambda_{x,m}$ and those of $g_v L_v^*$ by $\lambda_{v,m}$. With a slight abuse of notation we also consider these eigenvalues to be functions $\lambda_x(\phi)$ and $\lambda_v(\phi)$ of ϕ defined above. By using the m 'th eigenvector above to calculate $L_x^* w_m$ and $L_v^* w_m$ it is easy to show that:

Lemma 3.1.

$$\begin{aligned} \lambda_x(\phi) &= g_x \sum_{j=-2}^2 \rho_{x,j} \exp(\imath \phi j) = g_x \sum_{j=0}^2 [\alpha_{x,j} \cos(j\phi) + \imath \beta_{x,j} \sin(j\phi)], \\ \lambda_v(\phi) &= g_v \sum_{j=-2}^2 \rho_{v,j} \exp(\imath \phi j) = g_v \sum_{j=0}^2 [\alpha_{v,j} \cos(j\phi) + \imath \beta_{v,j} \sin(j\phi)]. \end{aligned} \quad (12)$$

The above equations are the discrete Fourier transform of the vectors ρ 's in Definition 3.3.

Let us now focus now on two eigenpairs of M_N^* [with the same definition as in Equation (6)] associated with w_m . Denoting the eigenvalues by $\nu_{m,\pm}$, we get:

$$\begin{pmatrix} 0 & I \\ g_x L_x^* & g_v L_v^* \end{pmatrix} \begin{pmatrix} w_m \\ \nu_{m,\pm} w_m \end{pmatrix} = \nu_{m,\pm} \begin{pmatrix} w_m \\ \nu_{m,\pm} w_m \end{pmatrix}. \quad (13)$$

For simplicity of notation we drop the subscripts of ν except when ambiguity seems possible. Evaluating second row of Equation (13), we get:

Lemma 3.2. *The eigenvalues of \mathcal{S}_N^* are given by the roots of the characteristic equation*

$$\nu^2 - \lambda_v(\phi)\nu - \lambda_x(\phi) = 0, \quad (14)$$

where $\phi = 2\pi m/N$.

Substituting the above expressions for λ 's, Lemma 3.1, we get:

$$\begin{aligned} \nu^2 - g_v \left[\sum_{j=0}^2 \alpha_v \cos(j\phi) + \imath \beta_{v,j} \sin(j\phi) \right] \nu \\ - g_x \left[\sum_{j=0}^2 \alpha_x \cos(j\phi) + \imath \beta_{x,j} \sin(j\phi) \right] = 0. \end{aligned} \quad (15)$$

Note that when $\phi = 0$, the characteristic equation becomes $\nu^2 = 0$. This gives two zero eigenvalues. These trivial eigenvalues are associated with the coherent solutions of the system, $z_k = 0$ (see also Equation 1).

4. Stability and signal velocities

Some necessary conditions for stability are derived and utilized to formulate our results for the signal velocities and their consequences. In this section we want to establish necessary and sufficient conditions, so that all other solutions of Equation (15) have negative real part, since as was explained in Section 2, this is one of the conditions for stability of the system.

Definition 4.1. *The collection \mathcal{S}^* is asymptotically unstable if at least one eigenvalue has positive real part.*

Note that collection \mathcal{S}^* is stable if 0 eigenvalue has multiplicity 2 and all other eigenvalues are smaller than 0 (see Lemma 3.2).

Lemma 4.1. *The following are necessary conditions for the collection \mathcal{S}^* not to be unstable:*

- (i) $\beta_{x,1} + 2\beta_{x,2} = 0$,
- (ii) $g_v \leq 0$,
- (iii) $\alpha_{v,1} \in [-4/3, 0]$,
- (iv) $g_x \alpha_{x,1} \geq 0$.

Proof: To prove (i) notice that the roots of characteristic Equation (14) are:

$$\nu_{\pm}(\phi) = \frac{1}{2} \left[\lambda_v(\phi) \pm \sqrt{\lambda_v(\phi)^2 + 4\lambda_x(\phi)} \right]. \quad (16)$$

For small ϕ , the λ 's can be approximated by their first order expansion. From Definition 3.4 and Lemma 3.1 we obtain:

$$\lambda_x(\phi \rightarrow 0) \approx ig_x \phi \sum_{j=0}^2 j\beta_{x,j}, \quad \lambda_v(\phi \rightarrow 0) \approx ig_v \phi \sum_{j=0}^2 j\beta_{v,j}. \quad (17)$$

Substituting these into equation for ν , Equation (16), we see that for small enough ϕ , the term $\pm\sqrt{4\lambda_x(\phi)}$ dominates. Since ϕ can be either positive or negative, this has four branches meeting at the origin at angles of $\pi/2$. Two of these branches contain eigenvalues with positive real part (for big enough N). Therefore, $\sum_{j=0}^2 j\beta_{x,j} = 0$.

For condition (ii) we note that the mean of the two roots of Equation (16) is equal $\lambda_v/2$. It follows that we must require $\Re[\lambda_v(\phi)] \leq 0$ for all $\phi \neq 0$. Since the average $\int \Re[\lambda_v(\phi)]d\phi$ is g_v , there is a ϕ so that $\Re[\lambda_v(\phi)] = g_v$. That of course means that g_v must be nonpositive. In turn, $\Re[\lambda_v(\phi)]$ is always nonnegative, therefore $\sum \alpha_{v,j} \cos j\phi \geq 0$. For the NNN system, the constraints on the α 's now give

$$1 + \alpha_{v,1} \cos(\phi) - (1 + \alpha_{v,1}) \cos(2\phi) \geq 0. \quad (18)$$

Since $\cos(2\phi) = 2\cos^2\phi - 1$, the inequality becomes a quadratic inequality in $\cos(\phi)$:

$$-(2 + 2\alpha_{v,1}) \cos^2(\phi) + \alpha_{v,1} \cos\phi + 2 + \alpha_{v,1} \geq 0, \quad (19)$$

which factors as:

$$-[(2 + 2\alpha_{v,1}) \cos(\phi) + 2 + \alpha_{v,1}] (\cos(\phi) - 1) \geq 0. \quad (20)$$

By working out three cases, $\alpha_{v,1} < -1$, $\alpha_{v,1} = -1$, and $\alpha_{v,1} > -1$, the conclusion of **(iii)** may be verified.

Beside $\phi = 0$, one other case of Equation (14) is easy, namely $\phi = \pi$ with the λ 's as defined in Lemma (3.1)

$$\nu^2 - \nu g_v \sum_{j=0}^2 (-1)^j \alpha_{v,j} - g_x \sum_{j=0}^2 (-1)^j \alpha_{x,j} = 0. \quad (21)$$

The roots have nonpositive real part if and only if both coefficients are nonnegative. In particular, this implies that last term in the above equation is $g_x \sum_{j=0}^2 (-1)^j \alpha_{x,j} \leq 0$. From Definition 3.4 we know that $\sum_{j=0}^2 \alpha_{x,j} = 1 + \sum_{j=1}^2 \alpha_{x,j} = 0$, and as a consequence $g_x \alpha_{x,1} \geq 0$, which is condition **(iv)**. Similarly, $g_v \alpha_{v,1} \geq 0$ but this already follows from conditions **(ii)** and **(iii)**. \square

Since we are interested in the parameter values for which the collection \mathcal{S}^* is not unstable, we use the above Lemma 4.1 and Definition 3.4 to eliminate a few parameters from our equations. This is done in the following definition.

Definition 4.2. *In the remainder of this work we will substitute $\beta_{x,2}$, $\alpha_{x,2}$, and $\alpha_{v,2}$ by setting:*

$$\beta_{x,2} = -\frac{1}{2}\beta_{x,1}, \quad \alpha_{x,2} = -(1 + \alpha_{x,1}), \quad \alpha_{v,2} = -(1 + \alpha_{v,1}). \quad (22)$$

Proposition 4.1. *If the collection \mathcal{S}^* is stable, the low-frequency expansion of $\nu_{\pm}(\phi)$ is given by*

$$\begin{aligned} \nu_{\pm}(\phi) = & \frac{i\phi}{2} \left[g_v(\beta_{v,1} + 2\beta_{v,2}) \pm \sqrt{g_v^2(\beta_{v,1} + 2\beta_{v,2})^2 - 2g_x(4 + 3\alpha_{x,1})} \right] \\ & + \frac{\phi^2}{4} \left[g_v(4 + 3\alpha_{v,1}) \pm \frac{g_v^2(\beta_{v,1} + 2\beta_{v,2})(4 + 3\alpha_{v,1}) + 2g_x\beta_{x,1}}{\sqrt{g_v^2(\beta_{v,1} + 2\beta_{v,2})^2 - 2g_x(4 + 3\alpha_{x,1})}} \right]. \quad (23) \end{aligned}$$

Proof: One can transcribe the first two terms of the corresponding expansion given in [17], or one can find the result by substituting power series in ϕ in Equation (15) or Equation (16). \square

This result immediately implies two other necessary criteria for stability. It is unclear whether together with the earlier criteria from Lemma 4.1 these constitute a necessary and sufficient set of criteria for the stability of \mathcal{S}^* .

Corollary 4.1. *The following are necessary conditions for the collection \mathcal{S}^* to not be unstable:*

- (i) $g_v^2(\beta_{v,1} + 2\beta_{v,2})^2 - 2g_x(4 + 3\alpha_{x,1}) \geq 0$,
- (ii) $g_v^2 g_x (4 + 3\alpha_{v,1})^2 (4 + 3\alpha_{x,1}) + 2g_v^2 g_x (\beta_{v,1} + 2\beta_{v,2})(4 + 3\alpha_{v,1})\beta_{x,1} + 2g_x^2 \beta_{x,1}^2 \leq 0$.

Proof: If condition **(i)** does not hold, then one branch of the first order expansion given in Proposition 4.1 will have positive real part. Condition **(ii)** corresponds to setting the argument of ϕ^2 in Proposition 4.1 as negative. \square

Theorem 4.1. *Suppose the collection \mathcal{S} is stable and flock stable. Then, under certain assumptions, as N (the number of agents) tends to infinity, the system \mathcal{S}_N will behave as a wave equation with signal velocities given by*

$$c_{\pm} = -\frac{1}{2}g_v(\beta_{v,1} + 2\beta_{v,2}) \pm \frac{1}{2}\sqrt{g_v^2(\beta_{v,1} + 2\beta_{v,2})^2 - 2g_x(4 + 3\alpha_{x,1})}. \quad (24)$$

Proof: The proof to a large extent is the same as the one given in the simpler case of nearest-neighbor presented in Reference [17]. \square

As a final comment in this section we want to point out that we are interested only in the cases where \mathcal{S} is flock and asymptotically stable. In other cases, the system can have dynamics not described by the methods used in this study. These cases can have interesting dynamics in their own right. An example of such a system is presented in Figure 3 with the configuration

$$\begin{aligned} g_x &= g_v = -2, \\ \rho_x &= (4/27, -289/432, 1, -253/432, 23/216), \\ \rho_v &= (47/216, -29/108, 1, -79/108, -47/216). \end{aligned} \quad (25)$$

\mathcal{S}_N^* with the above configuration is stable according to Definition 4.1. However, this does not imply stability of \mathcal{S}_N . In fact, although above configuration satisfies Lemma 4.1 and Corollary 4.1, the system \mathcal{S}_N has eigenvalues with positive part, and is therefore asymptotically unstable. It is evident from Figure 3 that presented results can not be modeled by simple traveling waves. However, we find that such a configurations - stable \mathcal{S}_N^* but unstable \mathcal{S}_N - are extremely rare.

5. Routh–Hurwitz stability criteria

Recall that we wish to establish conditions that guarantee that the system on the line is both asymptotically stable and flock stable. A direct verification of this might not be easy to perform. However, by the assumptions stated in Section 2, we can do this by finding the conditions that guarantee that the system on the circle is not unstable. Luckily this is a much simpler problem: we only need to show that roots of Equation (15) have real part less than or equal to zero.

The Routh-Hurwitz criterion is a standard strategy to derive a concise set of conditions that is equivalent to the fact that all roots of a given polynomial have negative real parts. In various systems similar to the ones discussed here, this criterion gives good results [17, 9]. In our current case the resulting equations are too complicated to give us much information and we only get one more necessary condition for stability that we can use (Corollary 4.1). Our discussion is based on Chapter 15, Sections 6, 8, and 13 of Ref. [21], where more details can be found.

Theorem 5.1. *(Routh-Hurwitz) Assume that the determinants given below are nonzero. Given a real polynomial $P = x^4 + a_3x^3 + a_2x^2 + a_1x + a_0$, all roots of P have negative real*

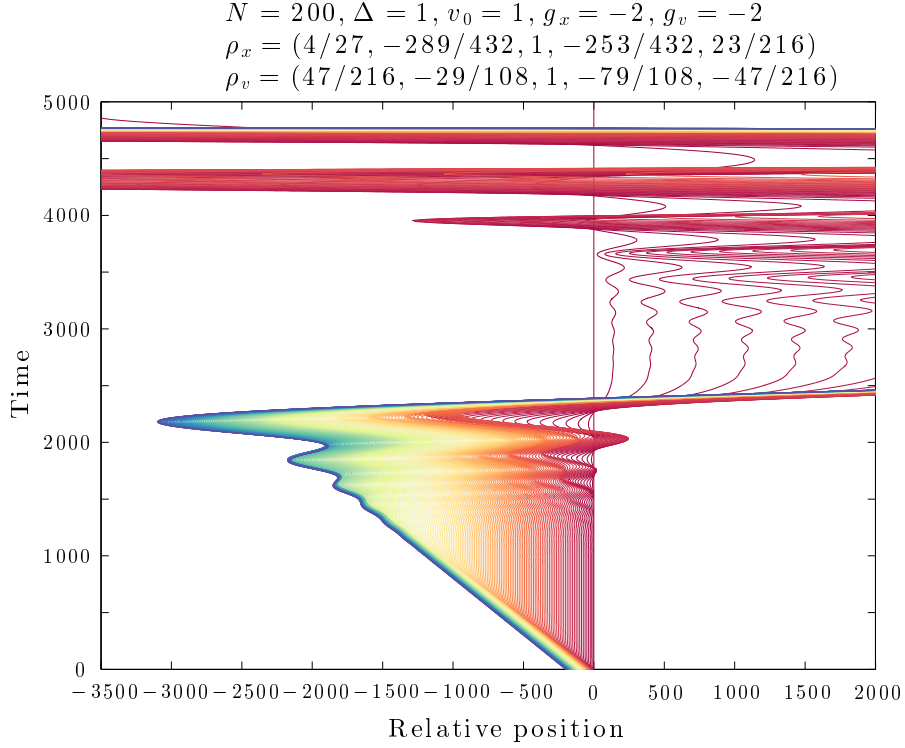


Figure 3. Dynamics of unstable system. Dynamics of example system \mathcal{S}_N as calculated for $N = 200$, $\Delta = 1$, $v_0 = 1$, $g_x = g_v = -2$, $\rho_x = (4/27, -289/432, 1, -253/432, 23/216)$, $\rho_v = (47/216, -29/108, 1, -79/108, -47/216)$ and fixed interaction BC. Each color represent the orbit of one of the 200 agents.

part if and only if all determinants of the upper-left submatrices (the leading principal minors) of:

$$A_4 \equiv \begin{pmatrix} a_3 & a_1 & 0 & 0 \\ 1 & a_2 & a_0 & 0 \\ 0 & a_3 & a_1 & 0 \\ 0 & 1 & a_2 & a_0 \end{pmatrix}, \quad (26)$$

are positive. That is: $a_3 > 0$, $a_0 > 0$, $a_3 a_2 - a_1 > 0$, and $a_3 a_2 a_1 - a_3^2 a_0 - a_1^2 > 0$.

An equivalent but less well-known set of conditions is given in the following:

Theorem 5.2. (Liénard-Chipart) Assume that the determinants in Theorem 5.1 are nonzero. Given a real polynomial $Q = x^4 + a_3 x^3 + a_2 x^2 + a_1 x + a_0$, all roots of P have negative real part if and only if $a_3 > 0$, $a_2 > 0$, $a_0 > 0$, and $a_3 a_2 a_1 - a_3^2 a_0 - a_1^2 > 0$.

The characteristic polynomial Q of Equation (15) can be turned into a polynomial with real coefficients

$$\begin{aligned}
QQ^* &\equiv \nu^4 - 2\Re(\lambda_v)\nu^3 + [|\lambda_v|^2 - 2\Re(\lambda_x)]\nu^2 \\
&\quad + 2[\Re(\lambda_x)\Re(\lambda_v) + \Im(\lambda_x)\Im(\lambda_v)]\nu + |\lambda_x|^2, \quad (27)
\end{aligned}$$

by taking its product with its complex conjugate. Clearly, all roots of Q have negative real part if and only if the same is true for QQ^* . Notice that in each of the two

criteria, one of the equations is trivially satisfied, namely $a_0 > 0$ (where we are assuming nondegeneracy). Therefore, in the Routh-Hurwitz case three equations are obtained. The first two are:

$$\Re(\lambda_v) < 0, \quad (28)$$

$$\Re(\lambda_v) [|\lambda_v|^2 - 2\Re(\lambda_x)] - [\Re(\lambda_x)\Re(\lambda_v) + \Im(\lambda_x)\Im(\lambda_v)] > 0. \quad (29)$$

The third inequality we do not utilize, since it is extremely complicated containing fifth order terms. We are left with the above two, which are now necessary conditions for all roots to have negative real part.

Similarly, the Liénard-Chipart stability criterion also gives two necessary conditions for all roots to have negative real part:

$$\Re(\lambda_v) < 0, \quad (30)$$

$$2\Re(\lambda_x) - |\lambda_v|^2 < 0. \quad (31)$$

The third inequality is the same as before and will not be utilized, as mentioned earlier. Since the second inequality of the Liénard-Chipart conditions seems less complicated than the corresponding one of the Routh-Hurwitz conditions, we will continue with the former.

Substituting the expressions for the λ 's (Lemma 3.1) we get:

$$(i) \quad g_v \left[\sum_{j=0}^2 \alpha_{v,j} \cos(j\phi) \right] < 0,$$

$$(ii) \quad g_x \left[\sum_{j=0}^2 \alpha_{x,j} \cos(j\phi) \right] - g_v^2 \left\{ \left[\sum_{j=0}^2 \alpha_{v,j} \cos(j\phi) \right]^2 - \left[\sum_{j=0}^2 \beta_{v,j} \sin(j\phi) \right]^2 \right\} < 0.$$

These are complicated relations therefore we will use the equivalent relations averaged over ϕ . The first of these equations was already used in Lemma 4.1. After some calculations we can work out the average over ϕ of the second relation. This gives the final necessary condition for all roots to have negative real part.

Corollary 5.1. *The following is a necessary condition for the collection \mathcal{S}^* to not be unstable:*

$$g_x - g_v^2 \sum_{j=-2}^2 \rho_{v,j}^2 \leq 0. \quad (32)$$

6. Solution classification

In Theorem 4.1 we saw that if \mathcal{S} is stable and flock stable, the systems \mathcal{S}_N will behave like a wave equation if N is large. This implies that transients will grow linearly in the number of agents of the flock. If these conditions are not met, then for N large, \mathcal{S}_N may be unstable or transients grow exponentially with the the size of the flock. Thus linear growth of transients cannot be improved for the type of the systems studied in this work.

Those solutions whose transients have linear growth, all resemble the solutions of a wave-like equation, namely they are approximately of the form $f_+(k-c_+t) + f_-(k-c_-t)$.

The constants c_- and c_+ are the signal velocities given by Theorem 4.1. Their units are in agent label per unit time. A positive velocity means going from the leader towards the last agent (labeled N). For the parameter values where this behavior occurs, the equation of motion Equation (3) behaves like a wave equation. If we choose other parameter values, transients will grow faster than linear and the behavior will be unlike the wave equation. Since the application we have in mind is flocking, we are interested in small transients. Accordingly, in this paper we limit ourselves to investigating the wave-like solutions only.

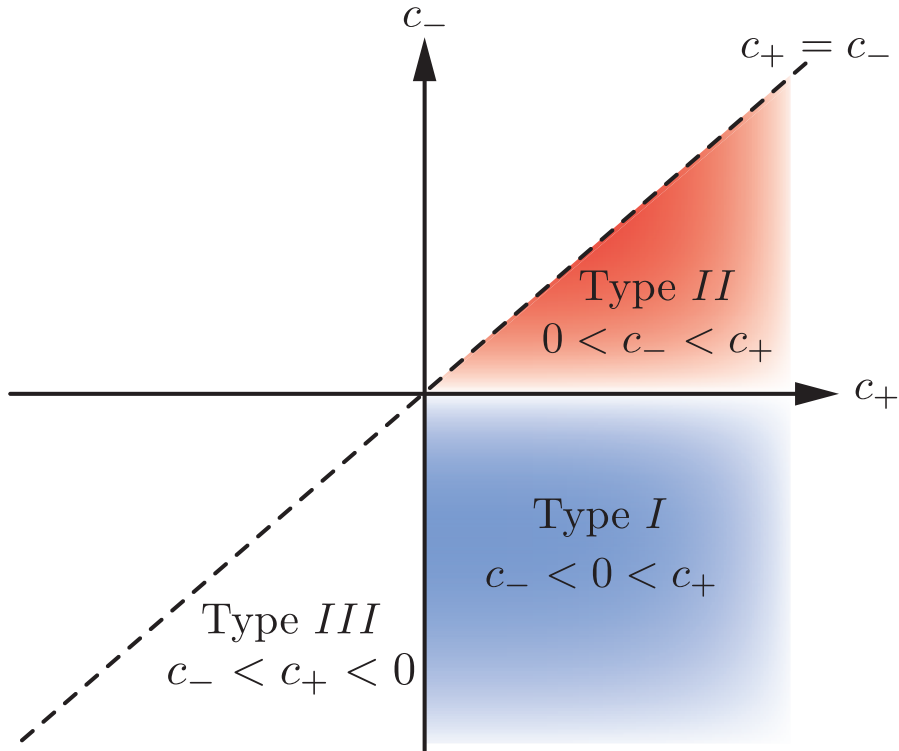


Figure 4. Phase diagram of signal velocities. Sketch of three type of solutions. Type I and Type II are stable with PBC and also on the line. Type III solution is stable only with PBC.

It turns out there are several types of wave-like solutions. These depend on the signs of the signal velocities c_{\pm} given in Theorem 4.1 - see the phase diagram presented in Figure 4. This is very different from the traditional physical, where signal velocities do not depend on direction. There are, in principle, three types of wave-like solutions. When $c_- < 0 < c_+$ the solutions resemble the traditional damped wave reflecting between the ends of the flock. This type of solution was already described in [18]. The difference in the signal velocities causes the wave to be damped (or magnified) when it reflects in agent N . These solutions are called Type I. When $0 < c_- < c_+$, that is the signal velocities are both positive, the wave cannot be reflected in the last agent, because it cannot move with negative velocity. Therefore these solutions are *reflectionless waves*. We also call these solutions Type II. It was proved in [18] that

such solutions cannot occur with only nearest-neighbor interactions. Finally, when $c_- < c_+ < 0$, the perturbation which in our set up starts at the leader, cannot be transmitted to the flock, because only negative signal velocities are available. Thus, another solution which does not appear to be wave-like, and which has very large amplitudes is found for the system (see Figure 7). The only reason for listing this solution in this work at all, is that if one looks at the system on the circle, wave-like solutions with negative signal velocities are indeed obtained. We call these solutions Type III. As with type II, these solutions cannot occur with only nearest neighbor interactions.

Note that in our analysis we ignore cases when $c_{\pm} = 0$ or $c_+ = c_-$. These cases are interesting by themselves, but have properties that make them undesirable for situations like traffic and other types of flocking. When $c_- = 0$, distances between agents do not tend to the desired distance Δ , but rather to some value that depends on the initial conditions. If $c_+ = c_-$, which on the line only occurs in Type II solutions, the velocity of the last agent is unbounded as N tends to infinity. We do not further investigate these solutions in this paper.

We now turn to the quantitative characterization of the trajectories of Type I and Type II (the ones with the smallest transients) for systems that are stable and flock stable. For large N one can show, based on the conjectures, that the orbit of the last agent is approximately piecewise linear. It can thus be effectively characterized by only a few parameters. For Type I, we characterize the orbit of the last agent [see Figure 2(a)] by the k 'th amplitude A_k , the period T , and the quotient $|A_{k+1}/A_k|$ which we refer to as the *attenuation* α . For Type II, we characterize the orbit of the last agent [see Figure 2(b)] by the amplitude A , the *first response time* T_1 and the *second response time* T_2 .

6.1. Type I: $c_- < 0 < c_+$

Theorem 6.1. *Suppose the collection \mathcal{S} is stable. Within Type I solutions the characteristics of the orbit of the last agent can be given by:*

$$\begin{aligned} A_k &= -v_0 N c_-^{k-1} / c_+^k, \quad \alpha = |A_{k+1}/A_k| = |c_-/c_+|, \\ T &= 2N(1/c_+ + 1/|c_-|), \end{aligned} \tag{33}$$

where A_k ($k \geq 1$) is the amplitude of $z_N(t)$ agent from its equilibrium position, α is the attenuation, and T is the oscillation period.

The proof to a large extent is the same as the one given in the simpler case of nearest-neighbor case [17].

In order to get optimal behavior, we want $|c_-/c_+| < 1$, so that the signal is attenuated. This means that in order to minimize transients, the emphasis should be placed on the upstream information in the velocity Laplacian.

Corollary 6.1. *If \mathcal{S} is asymptotically stable and flock stable then \mathcal{S}_N is of Type I and boundary effects will attenuate the signal if $(\beta_{v,1} + 2\beta_{v,2}) > 0$ and $g_x(4 + 3\alpha_{x,1}) < 0$.*

Proof: According to Theorem 4.1, c_{\pm} has a form $c_{\pm} = \frac{1}{2}(-a \pm \sqrt{a^2 - b})$, where $a = g_v(\beta_{v,1} + 2\beta_{v,2})$ and $b = g_x(4 + 3\alpha_{x,1})$. Since $c_- + c_+ > 0$, we see that $a < 0$ [see Lemma 4.1(ii)]. We also have that $c_- < 0$ thus $b < 0$. \square

These systems are typical examples of damped oscillations and we refer the interested reader to References [17, 18] for more detailed analysis of such solutions in the nearest-neighbor case. In Figure 5 we present exemplary dynamics of Type I stable system \mathcal{S}_N . For the presented configuration of ρ 's [$\rho_x = (-0.5, 0.25, 1, -0.75, 0)$ and $\rho_v = (-1, 0.75, 1, -1, 0.25)$] predicted characteristics are $A_1 = 80, \alpha = 0.4, T = 560$, where measured $A_1 = 77.179, \alpha = 0.3766, T = 567.63$.

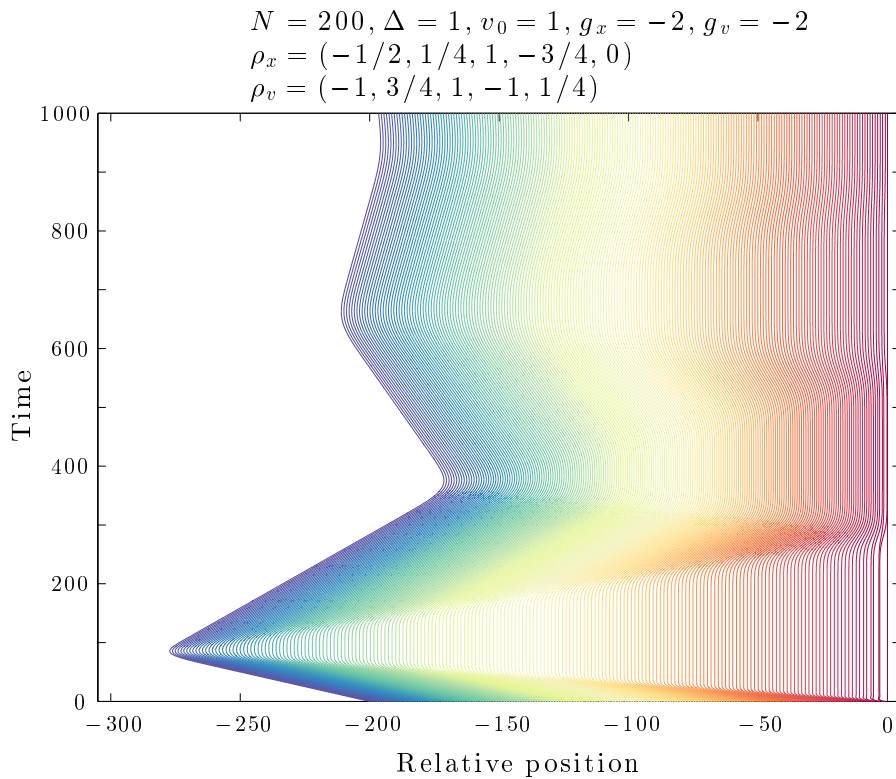


Figure 5. Dynamics of Type I solution. Dynamics of example system \mathcal{S}_N as calculated for $N = 200, \Delta = 1, v_0 = 1, g_x = g_v = -2, \rho_x = (-0.5, 0.25, 1, -0.75, 0), \rho_v = (-1, 0.75, 1, -1, 0.25)$ and fixed interaction BC. Each color represent the orbit of one of the 200 agents.

6.2. Type II: $0 < c_- < c_+$

Corollary 6.2. *Both of the velocities will be positive when $g_v(\beta_{v,1} + 2\beta_{v,2})$ is negative and $2g_x(4 + 3\alpha_{x,1})$ is positive, see Theorem 4.1.*

Proof: Similar to the proof of Corollary 6.1. \square

Within such a system, start signal travels from the leader to the last agent with velocity c_+ , and subsequently second signal velocity c_- stops the motion of the agents. A remarkable aspect of this type of solution is that very briefly after the second response

time, the trajectory of the last agent is almost exactly in its equilibrium position. Dynamics within such a system can be described as a traveling wave–package which does not reflect in the boundary of the system.

Theorem 6.2. *Suppose the collection \mathcal{S} is stable. Reflectionless waves can be characterized by*

$$A = -v_0 N / c_+, \quad T_1 = N / c_+, \quad T_2 = N / c_-, \quad (34)$$

where A is the amplitude and T_1, T_2 are first and second response time, respectively.

In Figure 6 we present typical dynamics of Type II stable system \mathcal{S} . For presented configuration of ρ 's ($\rho_x = (1, -2, 1, 0, 0)$ and $\rho_v = (-0.5, -1, 1, 0.5, 0)$) predicted characteristics are $A = 43.845, T_1 = 43.845, T_2 = 456.16$, where measured are $A = 43.182, T_1 = 43.182, T_2 = 453.95$.

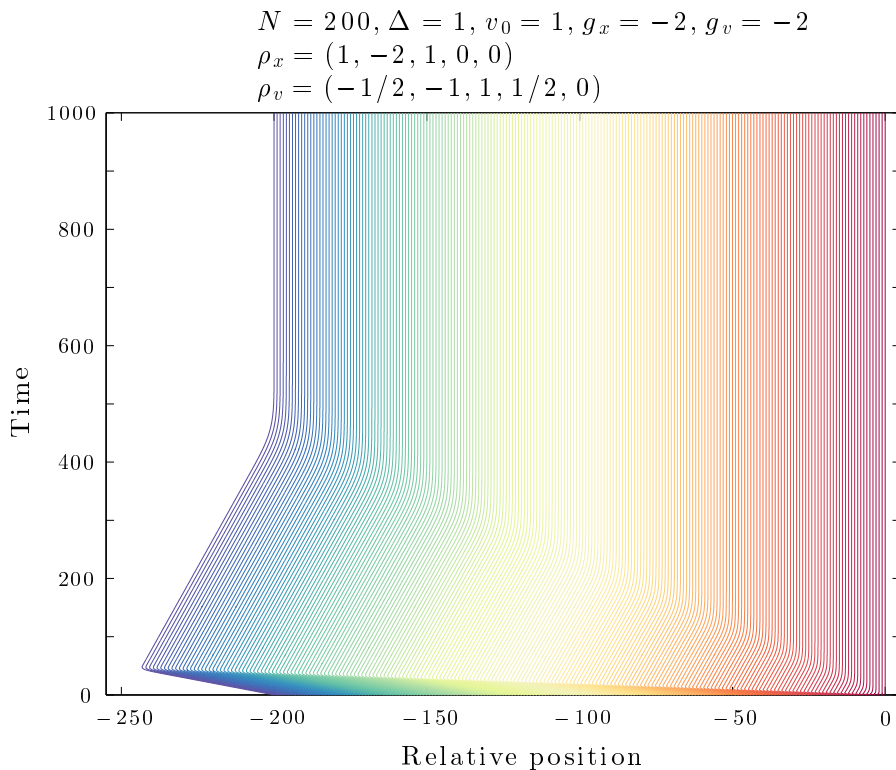


Figure 6. Dynamics of Type II solution. Dynamics of example system \mathcal{S}_N as calculated for $N = 200, \Delta = 1, v_0 = 1, g_x = g_v = -2, \rho_x = (1, -2, 1, 0, 0), \rho_v = (-0.5, -1, 1, 0.5, 0)$ and fixed interaction BC. Each color represent the orbit of one of the 200 agents.

The stable Type II solutions $z_k(t)$ appear to satisfy a condition

$$\forall t \geq 0 \quad \left. \frac{\partial}{\partial k} z_k(t) \right|_{k=0} = 0. \quad (35)$$

If we impose this theoretical boundary condition (as opposed to the physical BC introduced in the end of Section 2), similarly to what was done in Reference [18], we

can use it to derive an approximate solution for $z_k(t)$:

$$z_k(t) = \frac{c_+}{(c_- + c_+)} f\left(t - \frac{k}{c_+}\right) - \frac{c_-}{(c_- + c_+)} f\left(t - \frac{k}{c_-}\right), \quad (36)$$

where $f(t) = z_0(t)$ is a prescribed orbit of the leader. This solution is asymptotic in $N \rightarrow \infty$ and the relative errors tend to zero as N tends to infinity.

6.3. Type III: $c_- < c_+ < 0$

Corollary 6.3. *Both of the velocities will be negative when $g_v(\beta_{v,1} + 2\beta_{v,2})$ is positive and $2g_x(4 + 3\alpha_{x,1})$ is positive, see Theorem 4.1.*

Proof: Similar to the proof of Corollary 6.1. \square

In such a system, the perturbation emanates from the leader and wave-like solution could travel to the rest of the flock only if it had a positive velocity (c_{\pm} is measured in agent label per unit time). Therefore, it cannot have a wave like solution for a system on the line (system \mathcal{S}_N). However, it does exhibit wave-like solution for a system on the circle (system \mathcal{S}_N^*).

Within such a setup, on short time scales, the leader simply starts and other agents do not follow him. On larger time-scales, other phenomena may take place. One of the possibilities is that systems characteristics, e.g., amplitudes will constantly grow with time. Thus, the system should be flock unstable or even asymptotically unstable. However, due to the complicated nature of the stability conditions, we do not have a proof of this.

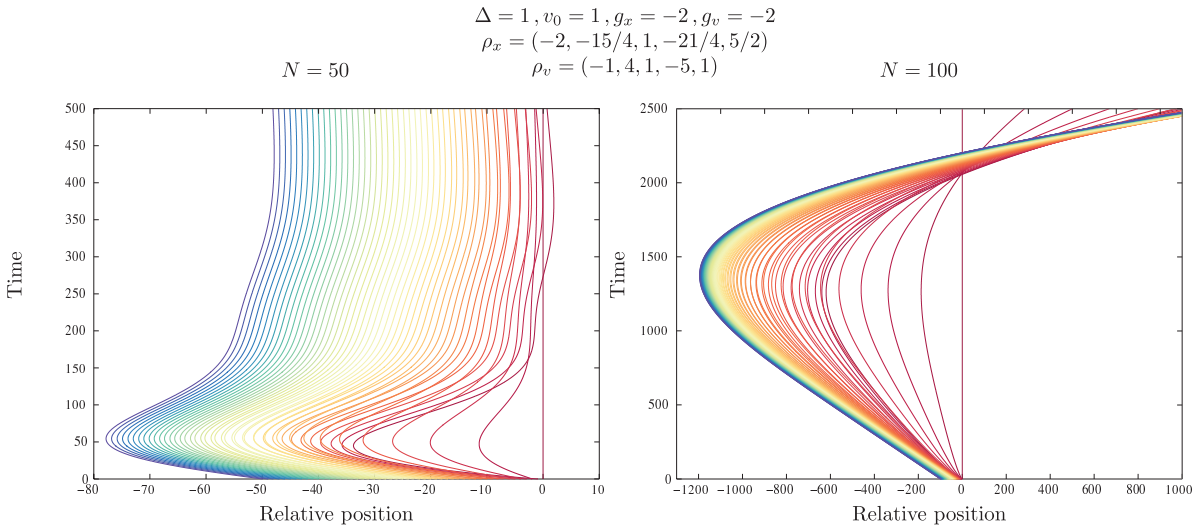


Figure 7. Dynamics of “Type III” solution. Dynamics of example system \mathcal{S}_N as calculated for $\Delta = 1, v_0 = 1, g_x = g_v = -2, \rho_x = (-2, -15/4, 1, -21/4, 5/2), \rho_v = (-1, 4, 1, -5, 1)$, fixed interaction BC $N = 50$ (left panel) and $N = 100$ (right panel). Each color represent the orbit of one of the 50 and 100 agents, respectively.

In Figure 7 we present a dynamics of the system \mathcal{S}_N whose solution on the circle

(system \mathcal{S}_N^*) is of Type III. It is obvious from presented results that, i.e., amplitudes do not grow linearly with system size.

7. Numerical tests

The parameter space $P \times B$ of the systems given in Definition 2.1 contains the 8-dimensional set P of values of g 's and ρ 's and the set B of boundary conditions (for NNN case B turns out to be a 11-dimensional). The obvious constraints for ρ 's are coming from Equation (4), i.e., consequence of decentralized system. By varying value of g 's and ρ 's, we generate sets P which contain $|P| \simeq 10^6$ unique system configurations p . We also characterize this set by type of solution (see Section 6),

$$P = P^I \cup P^{II}, \quad (37)$$

where superscript I and II correspond to Type I and Type II solution, respectively. It is worth noting that we did not find Type III solutions in our P . These appear to be quite rare, and in order to analyze them, we had to explicitly search for them (see Section 6.3).

Our aim is to numerically verify the set of conditions given in Lemma 4.1, Corollary 4.1 and Corollary 5.1, and for Type I only Corollary 6.1:

- (i) $\beta_{x,1} + 2\beta_{x,2} = 0$,
- (ii) $g_v \leq 0$,
- (iii) $\alpha_{v,1} \in [-4/3, 0]$,
- (iv) $g_x \alpha_{x,1} \geq 0$,
- (v) $g_v^2(\beta_{v,1} + 2\beta_{v,2})^2 - 2g_x(4 + 3\alpha_{x,1}) \geq 0$,
- (vi) $g_v^2 g_x (4 + 3\alpha_{v,1})^2 (4 + 3\alpha_{x,1}) + 2g_v^2 g_x (\beta_{v,1} + 2\beta_{v,2})(4 + 3\alpha_{v,1})\beta_{x,1} + 2g_x^2 \beta_{x,1}^2 \leq 0$,
- (vii) $g_x - g_v^2 \sum_{j=-2}^2 \rho_{v,j}^2 \leq 0$,

for subsets P^I , we required that (viii) $|c_-/c_+| < 1$.

Our test strategy is as follows:

- (1) For each configuration $p \in P^I$ and $p \in P^{II}$, we have checked the above conditions. The set of p 's which fulfill all of the conditions is denoted as P_{stable}^I and P_{stable}^{II} , correspondingly. The set of unstable configurations has a subscript “unstable”.
- (2) For each configuration $p \in P^I$ and $p \in P^{II}$, we evaluate the system with PBC and $N = 200$ agents, system $\mathcal{S}_{N=200}^*$, and calculate the eigenvalues of M_N^* . We denote as $\tilde{P}_{\text{unstable}}^I$, the collection of p 's for which in the eigenspectrum of M_N^* is at least one eigenvalue with positive real part or/and more than 2 zero eigenvalues, and it's complement as $\tilde{P}_{\text{stable}}^I$. We do the same for $\tilde{P}_{\text{unstable/stable}}^{II}$. Note that $\tilde{P}_{\text{stable}}^I$ and $\tilde{P}_{\text{stable}}^{II}$ is the collection of configuration p which are, according to Definition 4.1, asymptotically stable.

- (3) For each configuration $p \in P^I$ and $p \in P^{II}$, we evaluate the system with fixed interaction BC (see Section 2) and $N = 200$ agents, system $\mathcal{S}_{N=200}$, and calculate the eigenvalues of M_N of it. We denote as $\widehat{P}_{\text{unstable}}^I$ the collection of p 's for which in the eigenspectrum of M_N is at least one positive eigenvalue or/and more than 2 zero eigenvalues. We do the same for $\widehat{P}_{\text{unstable}}^{II}$. $\widehat{P}_{\text{stable}}^I$ and $\widehat{P}_{\text{stable}}^{II}$ is the collection of configuration p which are, according to Definition 3.1, asymptotically stable.

In our numerical investigation we have found that

$$\begin{aligned} P_{\text{stable}}^I &\equiv \widetilde{P}_{\text{stable}}^I \equiv \widehat{P}_{\text{stable}}^I, & P_{\text{stable}}^{II} &\equiv \widetilde{P}_{\text{stable}}^{II} \equiv \widehat{P}_{\text{stable}}^{II}, \\ P_{\text{unstable}}^I &\equiv \widetilde{P}_{\text{unstable}}^I \equiv \widehat{P}_{\text{unstable}}^I, & P_{\text{unstable}}^{II} &\equiv \widetilde{P}_{\text{unstable}}^{II} \equiv \widehat{P}_{\text{unstable}}^{II}, \end{aligned} \quad (38)$$

therefore, no exception was found. Note that, although our conditions are for \mathcal{S}_N^* not be unstable, they yield quite good predictions for stability of \mathcal{S}_N .

According to conjectures [17, 18] (see also discussion in Section 2) the BC do not play any role. In order to validate this we choose two $\text{BC} \in B$ introduced in Section 2. Also, as we saw in Section 6, measured values of certain characteristics presented for $N = 200$ differ slightly from the predicted ones, Theorem 6.1 and Theorem 6.2, by small value. This is expected, since our predictions are valid for $N \rightarrow \infty$. In order to test this, we choose 500 configurations from P_{stable}^I and 500 configurations from P_{stable}^{II} with period $T \lesssim \mathcal{O}(10N)$ and second response time $T_2 \lesssim \mathcal{O}(10N)$, respectively. We put this constraint for T and T_2 in order to decrease computation time of these configurations for large N . Then, we ran each of these configuration for $N \in \{25 \cdot 2^n\}_{n=0}^{n=11}$ and fixed interaction and mass BC. We use the ordinary differential equation solver of Boost library [22, 23] in a parallel computing environment. We measure the characteristics directly from numerical simulations and compare them with predictions of Theorem 6.1 and Theorem 6.2. In Figure 8 we present curves of *relative error* = $|measured - predicted|/|predicted|$, of averaged over N_{samp} configurations and maximal one of first amplitude A_1 , period T , and attenuation α for Type I solution, together with amplitude A , first T_1 and second T_2 response time for Type II solution.

As is clearly visible in Figure 8, the relative errors decrease as N grows, as is predicted by the theory. Our numerical analysis is consistent with the statement that - with the exception of period T for Type I orbit - the error decreases as $\mathcal{O}(1/\sqrt{N})$. The error in the period T (for Type I) appears to decrease as $\mathcal{O}(1/N)$.

8. Conclusions

We have investigated the dynamics of linearly coupled oscillators with next-nearest-neighbor interaction on the line. To our knowledge, it seems not possible - or at least very hard - to characterize the dynamics of this system by analyzing its equations of motion directly. Here we follow [17] and [18] and study the leaderless systems \mathcal{S}^* with periodic boundary conditions. The stability of this system, which is easier to establish, is found to be an effective criterion for the stability and flock stability of the systems

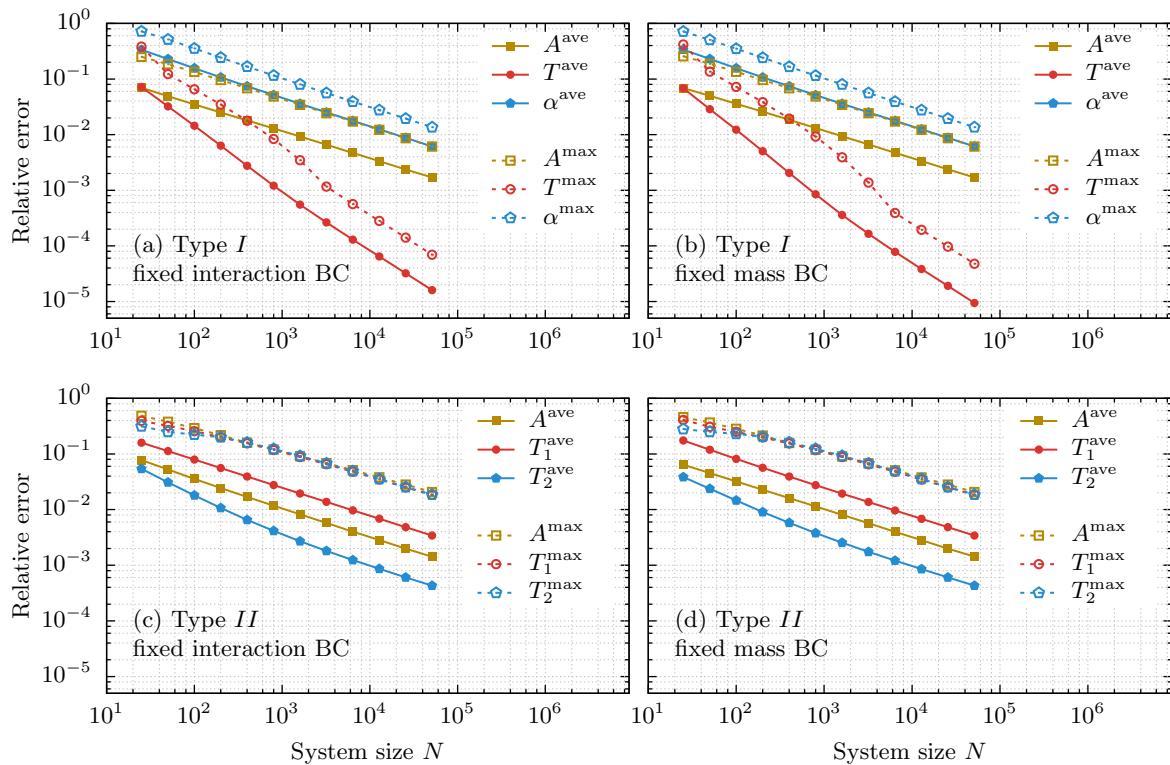


Figure 8. Relative error size scaling. Size N dependence of average and maximal relative error of Type I and Type II solutions for fixed interaction and mass boundary condition (see Definition 2.2) as calculated for $N = 25, \dots, 51200$ agents. Notice that the plot has log–log scale, therefore slope corresponds to the power of the decay.

on the line, \mathcal{S} . In addition it provides us with the tools to quantitatively completely characterize the transients of the system on the line.

Our results were numerically tested for two illustrative BC. However, the analysis presented is valid also for other BC, provided that the system can be successfully analyzed with PBC, and therefore for large enough N , boundary conditions do not influence the dynamics of the system.

Similarly to the case of nearest–neighbor systems [18], symmetric interactions are far from optimal and asymmetric cases show better performance. In fact the smallest transients tend to occur in the newly found type II solutions. In these wave-like solutions, the agents accelerate and decelerate *only once* to join the flock. There are, as it were, no reflections of these waves.

Wave-like behavior without apparent reflection was recently demonstrated experimentally to occur in flocks of starling birds [13, 24]. When the flock turns, the change of the heading of individual birds propagates through the flock in the wave-like fashion. This appears to happen in the same manner of our reflectionless waves: the heading of birds accelerates and decelerates only ones to assume its new value. The question arises whether the same mechanism discussed in this paper that gives rise

to reflectionless waves one-dimensional flocks, also operates in 2 and 3 dimension to generate wave-like solution. If that is the case, this mechanism could well operate in course changes of actual bird flocks. We leave this as a future challenge and motivation for further study.

Acknowledgments

We acknowledge support by the European Union's Seventh Framework Program FP7-REGPOT-2012-2013-1 under grant agreement no. 316165.

References

- [1] Lewis F L, Zhang H, Hengster-Movric K and Das A 2014 *Cooperative Control of Multi-Agent Systems: Optimal and Adaptive Design Approaches* (Dordrecht, Germany: Springer)
- [2] Backhaus S and Chertkov M 2013 *Physics Today* **May** 42
- [3] Motter A E, Myers S A, Anghel M and Nishikawa T 2013 *Nature Physics* **9** 191
- [4] Bamieh B, Paganini F and Dahleh M 2002 *IEEE Trans. Autom. Control* **47** 1091
- [5] Cruz D, McClintock J, Perteet B, Orqueda O, Cao Y and Fierro R 2007 *IEEE Control. Syst. Mag.* **27** 58
- [6] Defoort M, Floquet F, Kokosy A and Perruquetti W 2008 *IEEE Trans. Ind. Ele.* **55** 3944
- [7] Lin F, Fardad M and Jovanovic M R 2012 *IEEE Trans. Autom. Control* **57** 2203
- [8] Barooah P, Mehta P G P and Hespanha J J P 2013 *IEEE Trans. Autom. Control* **54** 2100
- [9] Herman I, Martinec D and Veerman J J P 2015 *arXiv: 1504.06075*
- [10] Reynolds C W 1987 *Comput. Graphics* **21** 25
- [11] Strogatz S H and Stewart I 1993 *Sci. Am.* **269** 102
- [12] Couzin I D, Krause J, Franks N R and Levin S A 2005 *Nature* **433** 513
- [13] Attanasi A, Cavagna A, Del Castello L, Giardina I, Grigera T S, Jelic A, Melillo S, Parisi L, Pohl O, Shen E and Viale M 2014 *Nature Physics* **10** 691
- [14] Pearce D J G, Miller A M, Rowlands G and Turner M S 2014 *Proc. Natl. Acad. Sci.* **111** 42
- [15] Trefethen L N, Trefethen A E, Reddy S C and Driscoll T A 1993 *Science* **261** 578
- [16] Trefethen L N 1997 *SIAM Rev.* **39** 383
- [17] Cantos C E, Veerman J J P and Hammond D K 2014 *arXiv: 1307.7143*
- [18] Cantos C E and Veerman J J P 2014 *arXiv: 1308.4919*
- [19] Ashcroft N W and Mermin N D 1976 *Solid State Physics* (Philadelphia, USA: Saunders College)
- [20] Veerman J J P, Caughman J S, Lafferriere G and Williams A 2005 *J. Stat. Phys.* **121** 901
- [21] Gantmacher F R 2000 *The Theory of Matrices* vol 2 (Providence, USA: American Mathematical Society)
- [22] Boost C++ libraries <http://www.boost.org>
- [23] Schöing B 2011 *The Boost C++ Libraries* (Laguna Hills, USA: XML Press)
- [24] Giardina I Personal communication